

Original Article

DOI 10.1007/s12206-021-0807-6

Keywords:

- Laser cleaning
- Mechanical grinding
- Aluminum alloy
- Microstructure
- Performance

Correspondence to:

C. M. Wang
cmwang@hust.edu.cn

Citation:

Li, Y., Wang, C., Mi, G. (2021). Influence of cleaning modes on the microstructure and performance of 5083 alloy substrate. *Journal of Mechanical Science and Technology* 35 (9) (2021) 3943~3949. <http://doi.org/10.1007/s12206-021-0807-6>

Received December 22nd, 2020

Revised May 7th, 2021

Accepted June 2nd, 2021

† Recommended by Editor
Chongdu Cho

Influence of cleaning modes on the microstructure and performance of 5083 alloy substrate

Yunkai Li, Chunming Wang and Gaoyang Mi

State Key Laboratory of Materials Processing and Die and Mould Technology, Huazhong University of Science and Technology, Wuhan 430074, China

Abstract In this study, the paint layer was removed on the surface of 5083 aluminum alloy using laser cleaning and mechanical grinding. The microstructure and performance of experimental samples were carefully investigated using scanning electron microscope, energy disperse spectroscopy and other methodologies. The results showed that compared with mechanical grinding, laser cleaning can improve the surface paint coating of aluminum alloy more effectively. The surface of the matrix formed uniformly distributed volcanic craters and small holes emerged at the spot junction after laser cleaning. The carbon and oxygen content on the substrate surface after laser cleaning was much lower than that after mechanical grinding. In addition, the corrosion resistance and coating adhesion of the substrate were obviously improved using laser cleaning. It was closely associated with refinement of the grains and reduction in surface roughness. We concluded that laser cleaning can be widely used to replace mechanical grinding in manufacturing on the premise of meeting industrial needs.

1. Introduction

5083 aluminum alloy is widely used in ships, aircraft parts and missile parts due to its medium strength, good corrosion resistance, excellent welding performance, low density and good cold workability [1, 2]. In view of complicated service environment, it is very necessary to paint the surface of aluminum alloy to extend the service life of parts [3]. However, with increasing the service time, local peeling or discoloration occurred in the paint layer, seriously affecting the service of parts. Therefore, it is imperative to remove the old paint layer and recoat the aluminum alloy surface, aiming at extending the service life of components [4].

Traditional paint removal methods consist mainly of sandblasting, chemical paint removal and mechanical paint removal [5]. During the removal process, it is easy to cause environmental pollution, endanger human health and damage metal substrates. Thus, in order to solve these problems [6], a new approach to remove old coatings becomes an urgent need.

Laser cleaning is a new technology based on the interaction between laser and matter [7]. During this process, the surface dirt, rust or coating can absorb the laser and instantly evaporate so as to achieve surface dirt removal. Compared with traditional cleaning methods, it has attracted the attention of many scholars because it has the advantages of non-contact and no pollution to the environment [8, 9]. The initial cost of laser cleaning is higher compared with mechanical grinding. Its average cost will be reduced because of its high efficiency, low maintenance cost and long service life. The mechanical grinding requires frequent replacement of parts and additional manpower investment. The price advantage of laser cleaning will become greater and greater under the current situation of increasingly expensive manpower employment. Based on these advantages, laser cleaning technology has been widely applied in the restoration of cultural relics [10, 11], mold cleaning [12] and removal of aircraft skins [13].

In the past years, many investigations reported paint removal using laser cleaning. Tserevelakisa et al. [14] used acousto-optic monitoring technology to monitor the process of laser

cleaning black paint layer on marble and predicted laser cleaning effect based on the statistical data. Schweizer et al. [15] conducted laser cleaning the skin of an aircraft and the efficiency reached 7.4 m²/h. Iwahori et al. [16] performed performance tests of composite materials via removing the surface paint layer. The results showed that the tensile and compressive strength of composite materials did not change after laser cleaning. Jiang et al. [17] researched the change of substrate properties after laser cleaning pipeline paint layers, and found that band-shaped and cracked areas emerged on the cross section of the substrate, and the hardness slightly increased in the surface layer. Wang et al. [18] analyzed the products in the process of laser paint removal. The composition of micron-level particles was similar to that of lacquer, which was closely related to the vibration mechanism. The carbon content in nano-level particles has decreased by 50 %. Tan et al. [19] studied the effect of laser removal on the mechanical properties of the substrate, and found that the tensile properties of the samples did not change. Most researches on laser cleaning paint coatings focused on the influence of laser cleaning on the tensile strength, surface hardness of the substrate and the analysis of paint removal products. However, few researches on the bond between the substrate and the coating after paint removal have been reported.

In this study, two cleaning methods, including laser cleaning and mechanical grinding, were used to remove paint coating of 5083 alloy. The surface morphology and element distribution of the substrate were carefully investigated using scanning electron microscope together with energy disperse spectroscopy. Moreover, the surface roughness, corrosion resistance and coating adhesion were further researched to evaluate feasibility and verify advantages of laser cleaning.

2. Experimental procedure

In this study, 5083 aluminum alloy sheets with a thickness of 4 mm were used as experimental samples. The alloy surface was covered with a layer of black epoxy paint by manual spraying. It is allowed to stand for 24 hours in a 25 °C environment to obtain a dried paint layer. The thickness of paint coating was about 30 μm. The chemical compositions of aluminum alloy and epoxy paint are shown in Table 1.

Fig. 1 shows laser cleaning system. The system platform included a fiber laser source, a workbench and a motion control system. The motion control system can alter the scanning mode and scanning speed of the pulsed laser. The laser source used in the experiment was a pulsed laser with a wavelength of 1064 nm. The cleaning head involved a collimator and X-Y axis-linked high-speed scanning galvanometer. The main characteristics of laser source are shown in Table 2.

The experimental plates were cut into samples of 10·10 mm size by a wire cutting machine for subsequent processing and related properties testing. In a laser cleaning process, a single laser pulse was used to irradiate the surface of the paint layer and induce the paint layer to separate from the substrate due

Table 1. Chemical composition of 5083 aluminum alloy and epoxy paint (wt %).

Element	Mg	Si	Fe	Cu	Mn
5083	4.9	0.04	0.4	0.1	0.4
Element	Cr	Ti	Zn	Al	
5083	0.05	0.15	0.25	Bal	
Element	C	O	P	S	
Paint	54.60	39.14	0.35	4.91	

Table 2. Laser source characteristics.

Characteristic	Symbol	Value	Units
Source	–	Fiber laser adopting MOPA	-
Wavelength	λ	1064	nm
Nominal average power	P	120	W
Pulse frequency	F	1-2000	kHz
Pulse duration	τ	10-400	ns
Maximum pulse energy	Pe	1.8	mJ
Mode	TEM	00	-
	M ²	< 1.6	-
Focused spot diameter	D	≈ 40	μm

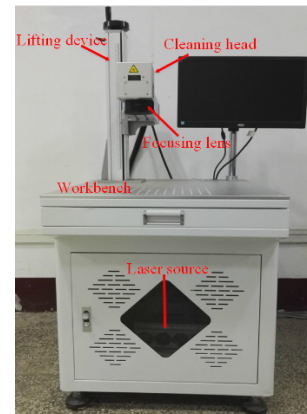


Fig. 1. Laser cleaning system.

to vaporization and thermal stress vibration. Fig. 2 shows the arrangement of laser spots along a certain direction. The distance d between two adjacent spots was determined by spot scanning speed v and laser repetition frequency f . The distance l between two adjacent linear spots equaled 0.03 mm.

As shown in Table 3, the main processing parameters contained average power P , spot diameter D , pulse width τ , laser repetition frequency f , spot moving speed v and number of scans n . In order to prove the effects of laser cleaning, comparative experiments were also performed on the experimental plates using mechanical grinding (180 molybdenum sandpaper).

The surface morphology of paint-removing samples was characterized by scanning electron microscope (SEM). EPMA-

Table 3. Experimental parameters.

P (W)	D (μm)	τ (ns)	f (kHz)	v (mm/s)	n
36	40	350	100	4000	3

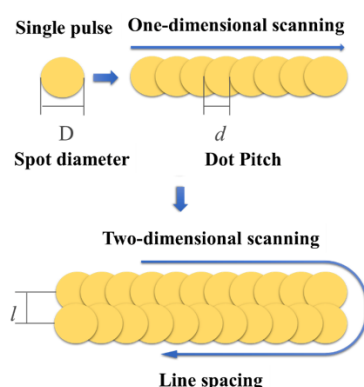


Fig. 2. Laser scanning and spot arrangement.

8050G electronic probe microanalyzer was also used to ascertain the elemental distribution of cleaned samples. The surface roughness of cleaned samples was determined using Form Talysurf PGI 830 surface profile comprehensive measuring instrument. The CS electrochemical workstation was used to characterize the corrosion resistance of cleaned samples. In addition, the bonding force between the coating and the substrate was tested by a multifunctional friction and wear tester.

3. Results and discussion

3.1 Microstructure of samples

Fig. 3 shows the micro-morphology of samples using laser cleaning and mechanical grinding. The surface of mechanical grinding sample mainly formed some defects including furrows, cracks and pits. During the grinding process, the furrow is generated parallel to the grinding direction because of the ploughing effect of silicon carbide particles on the surface of samples. Under the action of alternating contact pressure, the surface material gradually disappeared. Joining of silicon carbide particles and part of the matrix can be successfully achieved by the generated heat during this process. Part of the substrate can be taken away, resulting in forming pits [20].

After laser cleaning, the surface of the matrix had a uniformly distributed volcanic crater shape with some tiny holes. These holes were formed at the overlap of two light spots. Moreover, the number of holes in the longitudinal direction was more than that in the horizontal direction. The reason was that during laser irradiating process, high-density energy made the matrix melt and vaporize rapidly, leading the occurrence of splash on the surface of molten pool [21]. The action time of pulsed laser is so short that the molten pool rapidly cooled and solidified. It had solidified before the splashed metal liquid spread on the metal surface, which formed a surface hole.

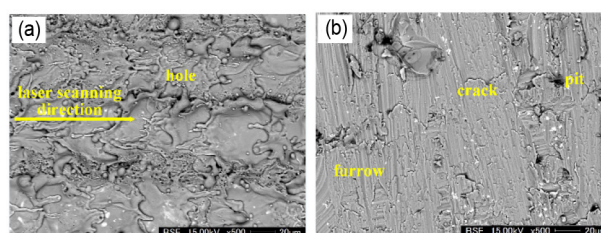


Fig. 3. Microstructures of cleaned samples: (a) laser cleaning; (b) grinding.

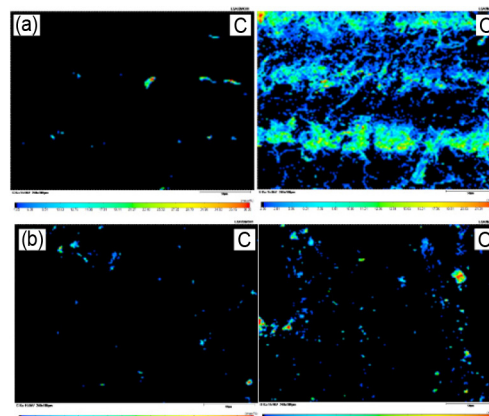


Fig. 4. Distribution of C and O elements on the surface of substrate and lower oxygen content after laser cleaning: (a) laser cleaning; (b) grinding.

3.2 The element distribution of samples

Fig. 4 shows the distribution of C and O elements on the surface of cleaned samples. After laser cleaning, the carbon content of the matrix surface was basically zero. Only a small amount of carbon was present at the longitudinal overlap of light spot.

There are two types of laser cleaning paint mechanisms involving the ablation mechanism and the vibration peeling mechanism. The ablation mechanism mainly uses high energy of the laser to vaporize the paint layer from the surface of the substrate. The vibration peeling mechanism is the thermal stress generated by the laser acting on the paint surface, causing the film to break and buckle away from the substrate surface [22]. The product is mainly micron particles. The low energy at the edge of laser spot prompts the emergence of the particle product, resulting in increasing the carbon content. A small amount of carbon elements remains on the surface of the aluminum alloy after mechanical grinding. Grinded paint powder particles are detained in the cracks and pits, so the surface carbon elements present a discrete distribution.

The oxygen element distribution of the matrix surface is affected by laser scanning method. In a laser cleaning process, part of laser energy removes the paint layer and excess energy acts on the surface of the aluminum alloy substrate so as to remove part of the oxide layer on the surface. The energy of the pulse laser is the Gaussian distribution. The center energy is higher than that at the edge, so the aluminum oxide layer at the center of the laser spot is almost completely removed while

Table 4. Aluminum alloy surface roughness after grinding and laser cleaning.

Surface roughness (Ra)						
Sample	1	2	3	4	5	Average
Grinding	1.14	1.36	1.70	1.26	1.03	1.30
Laser cleaning	0.94	0.86	1.25	1.18	1.09	1.06

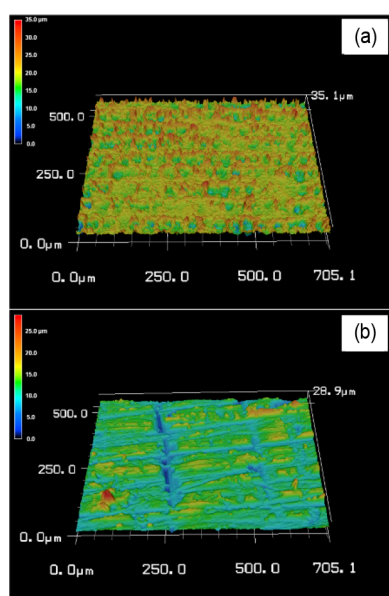


Fig. 5. The 3D morphology of aluminum alloy: (a) laser cleaning; (b) grinding.

the oxide layer at the spot overlap is only partially removed. Therefore, the distribution of oxygen element on the surface of the matrix is distributed in a parallel band shape. It can be also found that the oxygen content in the center of the spot is lower than that in the spot overlap. The reason is that the occurrence of higher oxygen content on the surface using mechanical grinding is the incomplete removal of oxide film.

3.3 Surface roughness of samples

Table 4 shows the surface roughness of the aluminum alloy after two different methods of paint removal. The value using mechanical grinding was Ra1.30, while the value employing laser cleaning was Ra1.06.

Compared with laser cleaning, the roughness amplitude of the aluminum alloy surface greatly fluctuated using mechanical grinding. Fig. 5 shows the 3D morphology of the cleaned and grinded aluminum alloy surface. When the laser acts on the aluminum alloy surface, a trough formed at the center of the spot because of higher energy while a wave peak appeared at the edge of the spot on account of lower energy. The roughness in cleaned surface had no significant fluctuations because the distance between adjacent peaks and valleys was almost constant. It mainly the ascribed same size and overlap rate of laser spot during the laser cleaning process. The furrows pre-

Table 5. Corrosion resistance of aluminum alloy using different cleaning methods.

	Self-corrosion potential (V)	Self-corrosion current density (A/cm ²)	Corrosion rate (mm/a)
Untreated	-1.35	1.64×10^{-4}	1.79
Grinding	-1.26	1.03×10^{-4}	1.12
Laser cleaning	-1.32	3.53×10^{-5}	0.386

sented a chaotic distribution in cleaned samples after mechanical cleaning. The deep furrow indicated that the aluminum alloy substrate has damaged. The silicon carbide particles had different forces on the surface of the aluminum alloy during grinding, resulting in an unevenly distribution on the aluminum alloy surface. After laser cleaning, the maximum height difference between the peak and the trough was 35.1 μm. However, the maximum height difference between the peak and the trough after mechanical grinding was 28.9 μm. In the laser cleaning process, larger splashes are occasionally generated after the substrate melts. These splash liquids solidify quickly and form higher peaks on the surface of the sample, but in most cases such splashes will not occur. So it is not contradictory to have a smaller surface roughness Ra and a larger maximum height difference after laser cleaning.

3.4 Corrosion resistance of samples

The corrosion resistance has a great impact on the service time of aluminum alloy in harsh environments. The electrochemical experiments were carried out to compare the corrosion resistance of cleaned samples with different treatment methods. Table 5 and Fig. 6 show the self-corrosion current density and corrosion rate of the aluminum alloy including raw materials, mechanical grinding and laser cleaning. The self-corrosion potential reflects the tendency of materials to corrode. The large negative the self-corrosion potential can mean that the material corroded easily. The self-corrosion current density reflected the corrosion rate of the material. The greater the self-corrosion current density, the higher the corrosion rate of the material.

It can be seen that the self-corrosion potentials of the untreated, mechanically grinded, and laser-cleaned substrates were -1.35 V, -1.26 V, and -1.32 V, respectively. Considering the test error, we considered that the corrosion tendency of the later material has not changed using mechanical grinding and laser cleaning. The corresponding self-corrosion current densities of these three samples were 1.63×10^{-4} A/cm², 1.03×10^{-4} A/cm² and 3.53×10^{-5} A/cm², using laser cleaning and mechanical grinding, improving the corrosion resistance of the aluminum alloy substrate to varying degrees.

According to the self-corrosion current density, the annual corrosion rate of the material can be obtained:

$$\text{Annual corrosion rate} = \frac{A \times I_{\text{corr}}}{n \times F \times \rho} \times 87600 (\text{mm/a}) \quad (1)$$

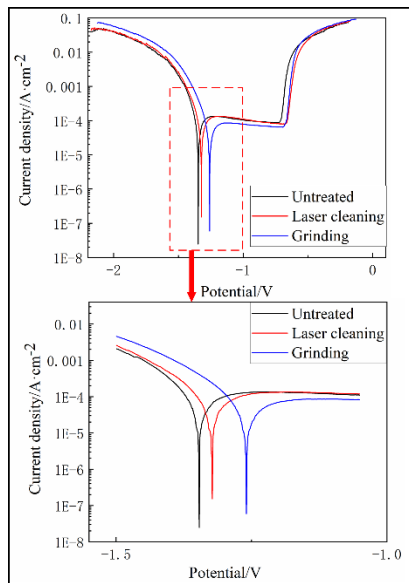


Fig. 6. Tafel curve of aluminum alloy using different paint removal methods in corrosion experiment.

where A is the relative atomic mass, $I_{\text{corr}}(\text{A}/\text{cm}^2)$ is the self-corrosion current density, n is the number of electrons transferred by the electrochemical reaction, F is the Faraday constant ($1 F = 26.8 \text{ A}\cdot\text{h}$) and $\rho(\text{g}/\text{cm}^3)$ is the density of the metal.

The corrosion rate of untreated aluminum alloy was 1.79 mm/a . After mechanical grinding, the corrosion rate of aluminum alloy was reduced to 1.12 mm/a , and the corrosion resistance was increased by 37 %. The reason was that mechanical grinding can remove the original defects such as pitting corrosion on the aluminum alloy surface while removing the paint layer, reducing the surface defects of the material and improving the corrosion resistance. The corrosion rate of aluminum alloy after laser cleaning was 0.386 mm/a . Compared with untreated samples, the corrosion resistance improved by 78 %. The surface grain size of the aluminum alloy decreased after laser cleaning. The grain size of aluminum alloy was refined and the number of active atoms inside the material increased. A passivation film was formed on the surface of the material, leading to the enhancement of the corrosion resistance of the material [23]. The surface roughness of the material also affected its corrosion resistance. The higher the surface roughness of the material, the smaller the electronic work function (EWF). The electrons were easily released on the surface of the material, leading to a higher corrosion rate [24]. Therefore, the corrosion resistance of the aluminum alloy substrate after laser cleaning was stronger than that after mechanical grinding.

In order to verify surface grain refinement after laser cleaning, EBSD test was performed on the aluminum alloy substrate. The average grain sizes were counted in the upper region and the entire region, respectively.

As shown in Fig. 7(b), the average grain size of entire region was $7.98 \mu\text{m}$ and the number of grains with less than $15 \mu\text{m}$

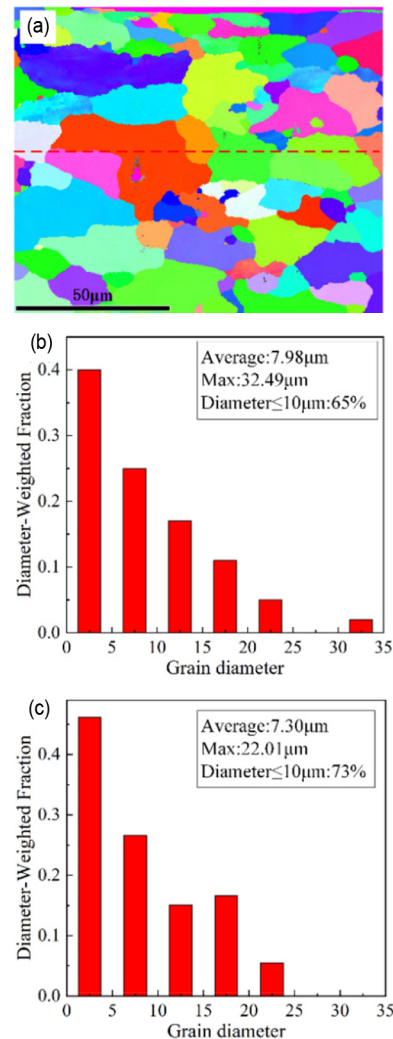


Fig. 7. Statistics of grain size of aluminum alloy substrate after laser cleaning: (a) EBSD results; (b) entire region; (c) upper region.

accounted for 65 % of the total. As shown in Fig. 7(c), the average grain size of upper region was $7.30 \mu\text{m}$ and the number of grains with less than $15 \mu\text{m}$ in diameter reached 73 % of the total. It proved that there was a certain grain refinement in the upper region.

3.5 Coating adhesion of samples

Fig. 8 shows the surface microstructure after scratch test. As the load increased, the groove width on the coating surface increased. In the initial stage, the surface coating damaged under the action of the indenter, but it did not break away from the surface of the substrate. As the load increased further, the coating completely separated from the surface of the substrate, exposing the bright white aluminum alloy substrate. We observed that comparing with mechanical grinding, the coating was separated from the surface using laser cleaning than. The bonding force between the surface and the coating using laser

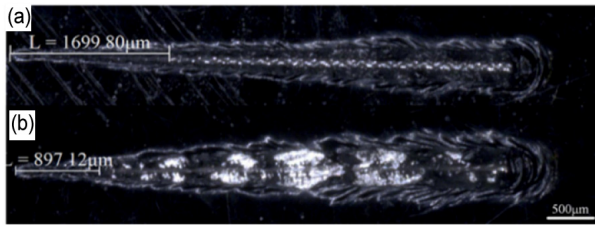


Fig. 8. The scratched position of coating in scratch test: (a) laser cleaning; (b) grinding.

treatment became higher.

The critical load was the load force when the paint layer broke. The coating adhesion can be obtained according to the formula.

$$\tau_A = \frac{K(H_V)\alpha}{\sqrt{R^2 - \alpha^2}}, \quad (2)$$

$$\alpha = \sqrt{\frac{P_c}{\pi(H_V)}} \quad (3)$$

where τ_A MPa was the coating adhesion in, P_c was the critical load in N, H_V was the substrate hardness in MPa, R was the scribing needle radius in mm, α was the scratch half width in mm and K was the constant, between 0.2 and 1.0.

After laser cleaning, the distance between the scratched position of the paint layer and the starting point was 1699.80 μm , corresponding to a critical load of 2.70 N. After mechanical grinding, the distance between the scratched position of the paint layer and the starting point was 879.12 μm , corresponding to a critical load of 1.88 N. Taking $K = 0.2$ [25], it was calculated that the adhesion force of the paint layer using laser cleaning was 14.18 MPa, and the adhesion force of the paint layer after mechanical grinding was 11.63 MPa. Comparing with mechanical grinding, the coating adhesion increased by about 22 % using laser cleaning.

The bonding strength between the substrate and the coating was related to the surface roughness of the substrate. A larger surface roughness induced the stress concentration more easily. The interface between the coating and the substrate subjected to greater shear force. The shear force can cause cracks in the surface coating. As the load increased, the coating layer cracks propagated. Finally, the coating was completely destroyed and separated from the surface of the substrate [26]. The surface roughness of the sample after laser cleaning is smaller. The coating is subjected to less shearing force when loaded with the same load, it is less prone to internal cracks and damage. The surface of the sample after laser cleaning has a stronger coating adhesion.

4. Conclusions

In this study, the microstructure and performance of 5083 aluminum alloys were carefully investigated using different

cleaning methods. The experimental results can be achieved as follows:

1) The surface of the aluminum alloy substrate formed uniformly distributed volcanic craters after laser cleaning. The small holes emerged at the spot junction because molten aluminum alloy liquid spatter failed to spread completely out over the surface under the action of the pulse laser.

2) After laser cleaning, the carbon element on the surface of the aluminum alloy had a small amount of residue at the longitudinal overlap of light spot and the distribution of oxygen element emerged in parallel bands.

3) Comparing with mechanical grinding, the corrosion resistance of the aluminum alloy substrate was obviously improved using laser cleaning. Increased corrosion resistance was closely associated with refinement of the grains and reduction in surface roughness.

4) The coating adhesion of samples was significantly increased using laser cleaning rather than mechanical grinding. It means that laser cleaning can completely replace mechanical grinding to remove paint in industrial production.

Acknowledgments

This work is supported by the National Natural Science Foundation of China (Grant No. 51861165202 and 51705173) and Science and Technology Planning Project of Guangdong Province (Grant No. 2017B090913001).

References

- [1] J. Paik, Mechanical properties of friction stir welded aluminum alloys 5083 and 5383, *International Journal of Naval Architecture and Ocean Engineering*, 1 (1) (2009) 39-49.
- [2] J. Cheng, Y. Huang and W. Dong, Experimental study on nanosecond laser cleaning of anodic oxide film of 5083 aluminum alloy, *Applied Laser*, 39 (1) (2019) 171-179.
- [3] W. Zhang, Technical status and application progress of marine coatings (part one), *Marine Equipment Materials and Marketing*, 2 (2008) 31-35.
- [4] A. Qian, P. Wang and X. Tan, Research on the aging failure of organic coatings and key technical issues, *Mechanical Science and Technology for Aerospace Engineering*, 36 (S1) (2017) 84-90.
- [5] B. Tian, W. Zou and Z. He, Pulsed Nd:YAG laser paint removal experiment, *Cleaning World*, 10 (2007) 1-5.
- [6] M. Zhao and J. Jing, Localization and application of coating system for high speed EMUs, *Modern Paint and Finishing*, 15 (9) (2012) 24-27.
- [7] Z. Lei, Z. Tian and Y. Chen, Laser cleaning technology in industrial fields, *Laser and Optoelectronics Progress*, 55 (3) (2018) 60-72.
- [8] D. Bauerle, Laser processing and chemistry: recent developments, *Applied Surface Science*, 186 (1-4) (2002) 1-6.
- [9] G. Daurelio, G. Chita and M. Cinquepalmi, New laser surface treatments: cleaning, derusting, deoiling, depainting, deoxidiz-

- ing, and degreasing, *Proc SPIE*, 3097 (1997) 369-391.
- [10] L. Zhang and H. Zhou, Application of laser cleaning technology in the protection and restoration of a female painted pottery figurine in han dynasty, *Sciences of Conservation and Archaeology*, 29 (2) (2017) 67-75.
- [11] X. Zhang, P. Zhang and C. Yang, Application of laser cleaning technology in the protection and restoration of a gilt bronze cultural relic, *Sciences of Conservation and Archaeology*, 25 (3) (2013) 98-103.
- [12] Z. Zhang, X. Yu and Y. Wang, Experimental study about cleaning of tire molds with pulse YAG laser, *Laser Technology*, 42 (1) (2018) 127-130.
- [13] G. Zheng, R. Tan and Y. Zheng, Experimental study on TEA CO₂ laser paint stripping, *Laser Journal*, 5 (2005) 82-84.
- [14] G. J. Tserevelakis, J. Santiago Pozo-Antonio and P. Siozos, On-line photoacoustic monitoring of laser cleaning on stone: evaluation of cleaning effectiveness and detection of potential damage to the substrate, *Journal of Cultural Heritage*, 35 (2019) 108-115.
- [15] G. Schweizer and L. Werner, Industrial 2 kW TEA CO₂ laser for paint stripping of aircraft, *Proceedings of Spie the International Society for Optical Engineering*, 2502 (1995) 57-62.
- [16] Y. Iwahori, T. Hasegawa and K. Nakane, Experimental evaluation for CFRP strength after various paint stripping methods, *Aeronautical and Space Sciences Japan*, 55 (2007) 235-240.
- [17] G. Jiang, P. Lei and Y. Liu, Laser removal of coating on oil and gas pipelines: effects on microstructure and hardness of substrate, *Chinese Journal of Lasers*, 47 (3) (2020) 167-174.
- [18] D. Wang, G. Feng and G. Deng, Study of mechanism on laser paint removal based on the morphology and element composition of ejected particle, *Chinese Journal of Lasers*, 42 (10) (2015) 115-121.
- [19] R. Tan, G. Zhen and Y. Zhen, The effect of laser paint stripping on the mechanical properties of the substrate, *Laser Journal*, 6 (2005) 83-84.
- [20] Y. Li, Q. Yue and H. Li, Friction and wear characteristics of 20Cr steel substrate and TiAlN coating under different lubrication conditions, *International Journal of Precision Engineering and Manufacturing*, 19 (10) (2018) 1521-1528.
- [21] G. Zhu, S. Wang and W. Cheng, Investigation on the surface properties of 5A12 aluminum alloy after Nd: YAG laser cleaning, *Coatings*, 9 (9) (2019) 578.
- [22] H. Zhao, Y. Qiao and X. Du, Laser cleaning performance and mechanism in stripping of polyacrylate resin paint, *Applied Physics A*, 126 (5) (2020) 360.
- [23] Y. Li and F. Wang, Effect of surface nanocrystallization on electrochemical corrosion behavior of metal materials, *Journal of Chinese Society of Corrosion and Protection*, 1 (2003) 6-8.
- [24] W. Li and D. Y. Li, Influence of surface morphology on corrosion and electronic behavior, *Acta Materialia*, 54 (2) (2006) 445-452.
- [25] X. Zhang, J. Chen and S. Liu, Bonding force test of multilayer oxide skin on high strength steel based on scratch test, *Materials Protection*, 51 (4) (2018) 125-129.
- [26] M. Furuno, K. Kitajima and Y. Tsukuda, Effect of ground surface roughness of tool on adhesion characteristics of PVD coating, *Advanced Materials Research*, 325 (2010) 315-320.



Yunkai Li is currently a master candidate student in Materials Processing Engineering at the Huazhong University of Science and Technology, Hubei, China. His research interests are in the area of paint removal using laser cleaning.